

1 



2
3
4 This document contains the **post-print pdf-version** of the referred paper:

5
6 **“Modeling the Effect of pH, Water Activity, and Ethanol Concentration on**
7 **Biofilm Formation of *Staphylococcus aureus*”**

8
9 by **Charles Nkufi Tango, Simen Akkermans, Mohammad Shakhawat Hussain,**
10 **Imran Khan, Jan Van Impe, Yong-Guo Jin and Deog Hwan Oh**

11
12 which has been archived on the university repository Lirias of the KU Leuven
13 (<https://lirias.kuleuven.be/>).

14
15 The content is identical to the content of the published paper, but without the final
16 typesetting by the publisher.

17
18 When referring to this work, please cite the full bibliographic info:

19
20 Nkufi Tango, C., Akkermans, S., Hussain, M., Khan, I., Van Impe, J., Jin, Y-G., Oh,
21 D-H. with Oh, D-H. (corresp. author) (2018). Modeling the Effect of pH, Water
22 Activity, and Ethanol Concentration on Biofilm Formation of *Staphylococcus aureus*.
23 *Food Microbiology* (76): 287-295.

24
25 The journal and the original published paper can be found at:

26 <https://doi.org/10.1016/j.fm.2018.06.006>

27
28 The corresponding author can be contacted for additional info.

29
30 Conditions for open access are available at: <http://www.sherpa.ac.uk/romeo/>

31

32

33

Modeling the Effect of pH, Water Activity, and Ethanol Concentration on

34

Biofilm Formation of *Staphylococcus aureus*

35

36

37

38

Charles Nkufi Tango^{1,2}, Simen Akkermans³, Mohammad Shakhawat Hussain¹, Imran

39

Khan¹, Jan Van Impe³, Yong-Guo Jin^{4**}, and Deog Hwan Oh^{1*}.

40

41

42

43

44

¹ Department of Bioconvergence Science and Technology, College of Agriculture and Life

45

Science, Kangwon National University, Chunchon, Korea. ² Department of Chemistry and

46

Agricultural Industries, Faculty of Agronomy, University of Kinshasa, Kinshasa, D.R. Congo.

47

³BioTeC, Chemical and Biochemical Process Technology and Control, Department of Chemical

48

Engineering, KU Leuven, Ghent, Belgium. ⁴National Research and Development Center for Egg

49

Processing, College of Food Science and Technology, Huazhong Agricultural University, Wuhan,

50

Hubei 430070, P. R. China.

51

52

53

54

55

56

*Author for correspondence. Tel: 82-33-250-6457; Fax: 82-33-241-0508; E-mail:

57

deoghwa@kangwon.ac.kr (Deog-Hawn Oh). **Co-author for correspondence. Tel: 86-27-8728-

58

3177; Fax: 86-27-8728-3177. E-mail: jinyongguo@mail.hzau.edu.cn (Yong-Guo Jin).

59

60 **Abstract**

61 In this work, the effect of environmental factors on *Staphylococcus aureus* (ATCC 13150)
62 biofilm formation in tryptic soy broth was investigated under different ranges of pH (3.0–9.5),
63 ethanol concentration (EtOH 0.0–20.0%), and a_w (NaCl, 0.866–0.992). Biofilm formation was
64 quantified using the crystal violet staining method and optical density (OD: 590 nm) measurements.
65 Biofilm formation was significantly stronger at pH and a_w close to *S. aureus* optimal growth
66 conditions, while it was high at EtOH around 2.5–3.5 %. Data sets from the difference between the
67 OD measurements of the test and control (Δ OD) were fitted to the cardinal parameter model (CPM)
68 and cardinal parameter model with inflection (CPMI) to describe the effect of the environmental
69 factors. The models showed a good quality of fit for the experimental data in terms of calculated
70 RMSE, with the latter ranging from 0.276 to 0.455. CPM gave a good quality of fit compared to
71 CPMI for the environmental factors tested. The optimal pH was close to neutral (6.76–6.81) and
72 biofilm formation was possible till pH = 3.81–3.78 for CPM and CPMI, respectively. Optimum
73 EtOH and a_w conditions for biofilm formation were in the range of 1.99–2.75 and 0.98–0.97,
74 respectively. Predicted OD values observed using strain 13150 were very closely correlated to the
75 OD values predicted with strain 12600 with R^2 of 0.978, 0.991, and 0.947 for pH, EtOH, and a_w ,
76 respectively. The cultivable bacterial cells within the biofilm were enumerated using standard plate
77 counting and a linear model was applied to correlate the attached biofilm cells to Δ OD of biofilm
78 formation. It was found that the biofilm formation was correlated with *S. aureus* population growth.
79 At 2.5–3.5% of EtOH the maximum population density was lower than that observed at 0.0% of
80 EtOH. As 2.5–3.5% of EtOH initiated a stronger biofilm formation, biofilm formation seems to be
81 induced by ethanol stress. The development of cardinal parameter models to describe the effect
82 environmental factors of importance to biofilm formation, offers a promising predictive
83 microbiology approach to decrypting the *S. aureus* population growth and survival ability on food
84 processing surfaces.

85

86 **Keywords:** *Staphylococcus aureus*, biofilm formation, pH, Water activity, Ethanol
87 concentration, Predictive microbiology.

88

89 **1. Introduction**

90 In natural and human-made ecosystems some bacteria have the ability to attach to surfaces
91 and form organized communities called biofilm. Its formation on food processing equipment leads
92 to the contamination of food products, which causes foodborne illnesses and significant economic
93 losses (Rode et al., 2007; Sharma and Anand, 2002). The microbial biofilm is a complex three-
94 dimensional structure composed of microbial cells and an extracellular matrix principally consisting
95 of polysaccharides, proteins, nucleic acids and lipids of microbial origin (Flemming and Wingender,
96 2010). These polysaccharides provide the structural scaffold of the biofilm and act as a shield against
97 various types of antimicrobials treatments (Arciola et al., 2012; Bridier et al., 2015). It has been
98 reported that contaminated surfaces play a pivotal role in spreading foodborne pathogens to food by
99 contact with food processing equipment and it is one of the main contributing factors to foodborne
100 outbreaks (Gormley et al., 2011; Perez-Rodriguez et al., 2013). It seems that biofilm formation is
101 essential for the bacterial survival on the food processing surface and poses a potential risk of post-
102 processing food contamination (Møretrø et al., 2003).

103 *Staphylococcus aureus* has the potential to colonize the surfaces of food processing
104 equipment and form biofilms. *S. aureus* has often been isolated from biofilms that developed in food
105 processing plant such as dairy, egg, seafood, and meat processing industries (Bridier et al., 2015;
106 Gutiérrez et al., 2012; Rohde et al., 2007; Shi and Zhu, 2009; Tango et al., 2015). The survival of
107 the *S. aureus* in hostile environments such as food processing equipment may be due to the biofilm
108 formation, which enhances the recurrence of planktonic bacterial populations when foods are
109 processed. Biofilms defy most antimicrobial agents and represent a potential source of bacterial
110 contamination in the food industry. It has been reported that *S. aureus* produces polysaccharide
111 intercellular adhesion (PIA) surrounding the cell, which can form a capsule and protects the bacterial
112 cell against host immune response (phagocytes) (Fox et al., 2005). Previous research has shown the
113 existence of a strong causal connection between staphylococcal biofilms and staphylococcal food
114 poisoning (SFP) through the consumption of staphylococcal enterotoxin (SE) produced in food (da
115 Silva Meira et al., 2012; Planchon et al., 2006). It is therefore essential for the food industry to
116 understand the conditions, under which *S. aureus* is able to survive, grow, and contaminate food

117 products with respect to biofilm formation. This knowledge is critical for a successful risk
118 assessment program.

119 Biofilm formation is a multistep process, involving a large number of physiological
120 changes in bacteria and takes place in response to environmental and biochemical factors
121 (Arrizubieta et al., 2004). The mechanism of staphylococcal biofilm formation in food industry and
122 on medical materials has been evaluated in detail and it is reported that *S. aureus* cells form biofilms
123 through various means. This ability to form a biofilm can be thwarted by the suboptimal growth
124 temperature and the presence of nitrite (Gustafson et al., 2014; Rode et al., 2007). However, sodium
125 chloride induces biofilm formation of *S. aureus* (Planchon et al., 2006). It has been reported that
126 alcohol can induce haemolytic properties in otherwise non-haemolytic microorganisms, a
127 phenomenon referred to as “microbial alcohol-conferred haemolysis” (MACH) (Korem et al., 2010;
128 Knobloch et al., 2001). Korem et al. (2010) demonstrated that alcohols selectively increased the
129 hemolytic properties of certain staphylococci strains and resulted in an increased biofilm formation.
130 Ethanol is commonly used as plant disinfectant in food industry, medical applications, and
131 household products, and hence may induce MACH on certain strains of *S. aureus*, thereby
132 increasing biofilm production when used at inappropriate concentration.

133 The transition from a planktonic to a complex three-dimensional structure is a dynamic
134 process that involves environmental and biochemical phenomena, thus is possibly implemented
135 through a developmental model (Hermanowicz, 2001; Monds and O’Toole, 2009). Considerable
136 effort has been employed during recent decades to develop mathematical models for describing
137 substrate use and microbial population dynamics during biofilm formation. Developed models, such
138 as individual-based models, successfully predict biofilm structure dynamics and clarify the
139 processes which govern biofilm formation and development (Bridier et al., 2015). The development
140 of new approaches of predictive microbiology may contribute to understanding the role of different
141 environmental conditions on biofilm development (Hermanowicz, 2001; Xavier et al., 2004). The
142 experimental methods will ultimately quantify the biofilm formation and mathematical models can
143 be useful tools for investigating the effects of different environmental factors on biofilm formation
144 by assumptions in which the enhancement or inhibitory effect of these factor is multiplicative (Ross
145 and Dalgaard, 2003). Regarding these aspects, this study was performed with the objective of

146 evaluating the *S. aureus* response to pH, ethanol concentration (EtOH), and water activity (a_w)
147 during switching between planktonic and biofilm modes and to develop a predictive microbiology
148 model to describe the effects of these environment factors on the biofilm formation ability of *S.*
149 *aureus*.

150

151 **2. Materials and Methods**

152 **2.1. Bacterial Strains for biofilm testing**

153 The modeling of biofilm development was performed using *S. aureus* strain ATCC 13150
154 and reference strain ATCC 12600 isolated from pork product and food processing environments.
155 Both strains were provided by the Department of Food Science and Biotechnology, Kangwon
156 National University, South Korea. The bacterial stock was maintained by cryopreservation at -80°C
157 in tryptic soy broth (TSB, Difco, Sparks, MD, USA) supplemented with 15% glycerol (Sigma-
158 Aldrich, Co, Saint-Louis, USA). Two days before each biofilm experiments, bacterial stocks were
159 thawed and recovered from deep freezing by spreading on Bard Park Agar (BPA, difco) and
160 incubated for 24 h at 37°C . Thereafter, single colonies were transferred in Brain Heart Infusion
161 (BHI, difco) broth and the culture was incubated overnight during a period of approximately 18 h
162 at 37°C , after which the overnight grown culture was used for the further biofilm development study.

163

164 **2.2. Experimental conditions**

165 The biofilm formation was studied in TSB (containing 0.5 % NaCl w/v) during a 48 h
166 incubation period at 37°C under different combination of a_w , pH, and ethanol concentrations. The
167 effect of NaCl concentrations was evaluated at concentrations of 2.5, 7.0, 10.0, 12.0, 14.0, 15.5,
168 17.0, 18.5, and 20.0 % (w/v) which correspond to a_w values of 0.983, 0.974, 0.961, 0.947, 0.934,
169 0.928, 0.911, 0.897, 0.887 and 0.861, respectively. TSB contained 0.5% of NaCl corresponded to
170 a_w value of 0.992. TSB a_w was determined with a_w -meter (Aquaspector AQS-2-TC, NAGY
171 Messysteme, Gäufelden, Germany) after adding NaCl to broth medium. The effect of pH was
172 studied in the range of 3.0 to 9.2 in step of 0.5 and adjusted in the broth medium using hydrochloric
173 acid (HCl 37%, Sigma, USA) or sodium hydroxide (NaOH, sigma, USA) with a digital pH meter
174 with an epoxy refillable pH probe (Thermo Electron Corporation, Beverly, MA, USA). Previous

175 studies have demonstrated that media supplemented with low concentrations of alcohols can
176 enhance staphylococcal biofilm formation (Korem et al., 2010; Knobloch et al, 2001). Therefore,
177 ethyl alcohol (Sigma, USA) was added to the TSB to produce final concentrations of 0.0, 1.0, 2.0,
178 3.5, 5.0, 7.0, 8.5, 10.0, 12.5, 15.0, and 20.0 % (v/v). The pH, EtOH, and a_w values in TSB were
179 measured before and after autoclaving to ensure that the abovementioned values were not
180 significantly changed. Before the biofilm experiments, the *S. aureus* ATCC 13150 overnight culture
181 was adjusted to an OD of 0.05 and 2.00 at 600 nm (Ependorff Biospectrometer fluorescence,
182 Hamburg, Germany) to obtain a concentration of approximately 5.0 and 8.0 log CFU/mL. This
183 inoculum level was confirmed by plating on TSA at 37°C for 24 h. Adjusted OD₆₀₀ of 2.00 was used
184 as initial inoculum for modelling the extent of biofilm formation and OD₆₀₀ of 0.05 for modeling
185 the relationship between biofilm formation and attached biofilm cells.

186

187 **2.3. Quantitative crystal violet biofilm assays**

188 Biofilm formation was evaluated using a colorimetric method which is based on the
189 measurement of the optical density (OD) of biofilms developed in polystyrene microtiter plate wells
190 (SPL Life Sciences, Pocheon, Korea) after crystal violet staining (Borucki et al., 2003; Djordjevic
191 et al., 2002). The OD₆₀₀ of 2.00 adjusted overnight culture was diluted (1:100) into TSB containing
192 the target conditions to be tested. A total of 200 µL of diluted TSB was distributed in a 96-well
193 plate. The plates were wrapped with parafilm and incubated for 48 h at 37°C, while TSB that was
194 not inoculated was also dispensed in wells and incubated (as a blank). Subsequently, the content of
195 the plate wells was discarded (removal of non-adherent or reversibly attached cells) and the wells
196 were gently washed twice with 225 µL autoclaved phosphate buffered saline solution (PBS, Sigma).
197 The plate wells were then emptied, air-dried and stained with 225 µL of 0.1% crystal violet (Difco
198 Laboratory, Detroit, USA) for 30 min. After rinsing off the excess stain with PBS twice and air-
199 drying of the microtiter plates, the crystal violet that was bound to the formed biofilms was dissolved
200 in 230 µL of 90% ethanol (Sigma) for 30 min, and the OD was measured at 590 nm using an
201 absorbance reader spectramax i3 (Molecular device, Sunnyvale, California, USA). The
202 quantification of biofilm formation was based on the difference between the OD measurements of

203 the test and blank plate wells (ΔOD). Reported data are based on five independent experiments
204 carried out with triplicate samples.

205

206 **2.4. Biofilm formation and sessile cells evaluation**

207 For attached biofilm cell enumeration, an overnight culture was adjusted to an OD of 0.05
208 at 600 nm to get approximately 5.0 log CFU/mL. The adjusted 24 h culture was transferred into
209 TSB (with 5 target conditions for each environmental parameter) as described above. Inoculated
210 TSB was dispensed in 96-well plate wells and incubated at 37°C for 6, 12, 18, 24, 30, 36, 42, and
211 48 h. The biofilm quantification was performed as described above and the number of cultivable
212 sessile cells was determined using standard plate counting as described by Hussain and Oh (2017).
213 Broth medium in the well was discarded and the plates were gently washed four times using 225 μ L
214 of PBS to remove unbound cells. Well plates were swabbed to detach the biofilm cells and the cell
215 suspensions were vigorously pipetted to separate biofilm cells from the swab in order to obtain
216 single cells. Serial dilutions were prepared in PBS and 0.1 mL of the appropriate dilution was plated
217 on TSA. Plates were enumerated after an incubation at 37 ± 2 °C for 24 h. Biofilm and cell counting
218 evaluations were performed in two replicate experiments on separate days for each condition tested.

219

220 **2.5. Model development**

221 **2.5.1. Modelling biofilm development**

222 To describe the individual effect of NaCl, pH, and ethanol on the *S. aureus* biofilm
223 formation, observed ΔOD values at different conditions of each factor were fitted to the cardinal
224 parameter models (CPM) and CPM with inflection (CPMI) to determine $\rho(X)$ for pH, a_w , and
225 ethanol concentrations according to equation (2) proposed by Rosso et al. (1995):

226

$$227 \quad \Delta OD = \Delta OD_{opt} \cdot \rho(X) \quad (1)$$

228

$$229 \quad X \leq X_{min}:$$

230

$$0$$

$$231 \quad X_{min} \leq X \leq X_{max}:$$

$$\rho(X) = \frac{(X - X_{max}) \cdot (X - X_{min})^n}{(X_{opt} - X_{min})^{n-1} \cdot [(X_{opt} - X_{min}) \cdot (X - X_{opt}) - (X_{opt} - X_{max}) \cdot (X_{opt} + X_{min} - nX)]} \quad (2)$$

$$X \geq X_{max}:$$

$$0$$

In equation (2) X_{min} and X_{max} are defined as the range of environment conditions where biofilm formation is possible, X_{opt} is the environmental condition where the optimum biofilm formation is observed, and n a curvature parameter ($n=1$, CPM and $n=2$, CPMI). Matlab version 9.2 R2017a (The Mathworks Inc. Natick, MA, USA) was used to determine the parameter estimates of the CPM and CPMI and for curve fitting (regression by the non-linear least squares method and the Trust-region algorithm). The calculation of the confidence bounds was based on the same equations as reported by Akkermans et al. (2017). A multi-start procedure was implemented to prevent finding a local optimum solution (100 iterations).

The developed models were evaluated using the goodness-of-fit statistic root mean square error (RMSE). The performance of developed model was assessed by graphical comparison between observed and predicted values and predictive performance factors (accuracy and bias factors).

2.5.2. Modeling the relationship between biofilm formation and attached biofilm cells

To describe the evolution of *S. aureus* populations in TSB during biofilm formation, the commonly used growth model of Baranyi and Roberts (1994) was implemented. The maximum growth rate (r_{max} , log cfu/well/h), lag phase (λ , h) and maximum population density N_{max} (log cfu/well) were estimated from the observed data at different conditions of pH, ethanol concentrations, and a_w using the DMFit version 2.1 Excel add-in software (Institute of Food Research, Norwich, England). Adjusted coefficient of determination (R^2_{adj}) and standard errors of the prediction (S_{xy}) were determined to assess the goodness-of-fit of the model. The re-parameterized Baranyi model, as the primary model, is described by the following equations:

$$N(t) = N_o + r_{max}A(t) - \ln \left[1 + \frac{e^{r_{max}A(t)} - 1}{e^{(N_{max} - N_o)}} \right] \quad (3)$$

259
$$A(t) = t + \frac{1}{r_{max}} + \ln\left(\frac{e^{r_{max}A(t)} + q_0}{1 + q_0}\right) \quad (4)$$

260
$$\lambda = \frac{\ln\left(1 + \frac{1}{q_0}\right)}{r_{max}} \quad (5)$$

261

262 With $N(t)$ the cell concentration (log cfu/well) for given time t (h), N_0 the initial and N_{max}
263 the maximum cell concentrations (log cfu/well), respectively, r_{max} the maximum growth rate (1/h).
264 $A(t)$ is an adjustment function described by Baranyi and Roberts (1994) and can be considered as a
265 rescaling of time, q_0 is the parameter expressing the physiological state of cell when $t=t_0$ (Eq. 4),
266 and λ is the lag time (h) (Eq. 5).

267 The cell concentration data of *S. aureus* in plate wells were fitted to a model proposed by
268 Castelijn et al. (2012) to evaluate the relation between the biofilm formation ability, as assessed
269 using the CV assay, and the concentration of cells attached on the wells' surface. The re-
270 parameterized model is described by the following equations:

271

272
$$A_{590} = a \cdot N + b \quad (6)$$

273

274 Were A_{595} is the absorbance of the solubilized CV after biofilm formation, N is the number
275 of viable attached biofilm cells (CFU/well), b is the background signal (three times the standard
276 deviation (SD) above the mean A_{595} of the negative control) and a is the proportionality constant
277 between CV staining and cell counts. The parameters a and b were estimated by fitting Equation 6
278 to the data using GraphPad Prism version 6.03 for windows (GraphPad Software, San Diego
279 California USA). The obtained parameters (a and b) were confirmed in Microsoft Excel by using
280 the Excel Solver add-in. The difference between kinetic growth parameters was analyzed through
281 an analysis of variance (ANOVA). Post-hoc tests (Tukey multiple range test) were used to determine
282 the statistical significance of differences between growth parameters ($p < 0.05$). All statistical
283 analyses were performed using SPSS statistics software version 22 (SPSS Inc., IBM Company,
284 USA).

285

286 **3. Results**

287 **3.1. Modelling *S. aureus* biofilm development**

288 Initially, 25 strains isolated from different food products and plants were evaluated to select
289 the highest biofilm producer. The evaluation was performed in TSB at 37°C for 48 h in polystyrene
290 microtiter plates. Among these strains, ATCC 13150 produced the strongest biofilm (data not
291 shown). *S. aureus* 13150 was studied in more detail as a target strain while investigating the effect
292 of pH, EtOH, and a_w on the biofilm formation in TSB at 37°C after 48 h of incubation in 96-well
293 microtiter plates. The biofilm formation was significantly stronger when pH and a_w were near the
294 *S. aureus* growth optimal conditions. While the biofilm formation was high at EtOH around 2.5–3.5
295 %. Two predictive microbiology cardinal parameters models were used to describe the effect of pH,
296 EtOH, and a_w on *S. aureus* biofilm development. Experimental data were collected from 225 biofilm
297 formation trials to model the influence of pH on biofilm formation of *S. aureus*. The pH effect was
298 evaluated at a_w of 0.992 and 0.0 % of EtOH concentration. The effect of pH on the biofilm formation
299 ability of strain 13150 is shown in Fig. 1A. The results demonstrated that *S. aureus* biofilm
300 formation depended strongly on pH variations. A very weak biofilm formation was observed at pH
301 values lower than 4.0 and higher than 9.0. Parameter estimates and 95% confidence intervals of
302 CPM and CPMI for pH are presented in Table 1. There was no difference between the estimate
303 parameters from CPM and CPMI for pH. The slight difference of RMSE observed between CPM
304 and CPMI showed that there is no inflection at suboptimal pH.

305 To model the effect of EtOH on biofilm formation, 155 experiments were performed at a_w
306 of 0.992 and pH of 7.0. The biofilm formation was highest at an EtOH concentration of 3.5. The
307 two model structures CPM and CPMI were also used to describe this effect and the fitted models
308 are graphically shown in Fig. 2A and 2B, respectively. The RMSE value was lower in CPMI (0.276)
309 than that observed in CPM (0.327). This illustrated that the quality of fit is greatly improved by
310 including the inflection for high EtOH concentrations. The estimated parameters were higher in
311 CPMI compared to those found in CPM for EtOH, except for the parameter $E_{th_{min}}$. However, there
312 is no true minimum ethanol concentration for biofilm formation and consequently the parameter
313 $E_{th_{min}}$ is given a theoretical negative value. Consequently, this parameter has no interpretation.

314 To model the effect of a_w using NaCl concentration on the biofilm formation, 155
315 experiments were performed at a pH of 7.0 and 0.0% of EtOH. Both curvature parameter $n=1$ and
316 $n=2$ were performed to describe the effect of this factor and the fitted models are graphically
317 displayed in Fig. 3A and 3B, respectively. The estimate parameters for CPM were almost equal to
318 those observed for CPMI for a_w . RMSE value was lower in CPM (0.276) compared to that calculated
319 in CPMI (0.327), demonstrating the better quality of fitting of the former compared to the latter
320 model.

321

322 **3.2. Validation**

323 The validation of cardinal models was performed using a goodness of fit statistics and
324 prediction accuracy indices. Firstly, to obtain a measure for the agreement between the experimental
325 data and the developed cardinal models, the experimental data were plotted against predicted data
326 using a linear regression. The average coefficient of determination (R^2) values were 0.918 for CPM
327 and 0.86 for CPMI, suggesting that the correlation between experimental data and predicted data
328 were better for CPM than CPMI for all factors used in the present study (Fig. 4). The accuracy factor
329 A_f and bias factor B_f were also calculated for both CPM and CPMI and each influencing factor. The
330 results of A_f and B_f are summarized in Table 1. The cardinal models performed well for these
331 datasets with average A_f of 1.107 and 0.996 and B_f of 1.273 and 1.320, respectively for CPM and
332 CPMI. In general, the accuracy and bias factors were acceptable as described by (Ross, 1999).

333

334 **3.3. Modeling the correlation between planktonic cells and biofilm formation**

335 To investigate the growth of biofilm attached populations during biofilm formation, 5
336 conditions for each factor (pH, EtOH, and a_w) were selected among the described conditions used
337 to study biofilm formation. The Baranyi and Roberts (1994) model was fitted to the population
338 counts and growth parameters were presented in Table 2. To model the correlation between the
339 biofilm attached *S. aureus* population and biofilm formation, the datasets were fitted to a linear
340 model to determine the factor a . The factor a represents a proportionality constant between the
341 attached *S. aureus* biofilm populations and OD observed. The linear model was graphically shown
342 in Fig. 5 and factor a was presented in Table 2. The results showed that the factor a from the linear

343 model was higher in TSB at pH 7.0 ($a = 2.85 \times 10^{-6}$) compared to those observed in TSB at pH 4.0
344 and 9.5 ($a = 7.88 \times 10^{-8}$ and $6.59 \cdot 10^{-8}$). The growth parameters r_{\max} and N_{\max} were higher in TSB with
345 pH 7.0 compared to those found for pH 4.0 and 9.5. Similar results were observed when biofilm
346 formation was studied in TSB supplemented with different concentrations of NaCl. The factor a
347 was higher at the optimal growth condition than suboptimal growth conditions. These results suggest
348 that the biofilm formation is correlated with *S. aureus* population growth (Castelijn et al., 2012;
349 Kadam et al., 2013). For EtOH, the results showed that N_{\max} (9.45 log cfu/well) was higher at TSB
350 without ethanol compared to those found in TSB supplemented with 3.5 and 7.0 % of ethanol (8.84
351 and 8.91, respectively). Moreover, the factor a was higher ($a = 3.55 \cdot 10^{-6}$ and $2.91 \cdot 10^{-6}$) for the
352 developed model for results in TSB supplemented with 3.5 and 7.0 %, respectively, compared to
353 that found in TSB with 0.0 % of ethanol. These results indicate that the extracellular matrix
354 production did not only depend on the *S. aureus* population growth but also on stress induces by
355 ethanol at the non-lethal concentration.

356

357 **4. Discussion**

358 *S. aureus* has been recognized as one of the greater biofilm producer bacteria and the
359 connection between staphylococcal biofilm and staphylococcal food poisoning has been previously
360 established (da Silva Meira et al., 2012; Planchon et al., 2006). In the present study, the effect of
361 environmental parameters on *S. aureus* biofilm formation was modeled using CPM and CPMI for
362 pH, EtOH, and a_w . The cardinal parameters are a family of models which define cardinal values
363 (minimum, optimum and maximum) of environment factors (temperature, pH, a_w , organic acids
364 ...) from the microbial growth rates observed at optimal or non-optimal conditions for other
365 environmental factors (Rosso et al., 1995). The CPMI was designed first to describe the effect of
366 temperature on microbial growth rate (Rosso et al., 1993). CPM was later extended to other
367 environmental factor including pH and a_w (Rosso et al., 1995; Rosso and Robinson, 2001). These
368 models are commonly used to describe and to predict the effect of environment factors on microbial
369 growth because they are based on parameters that are biologically meaningful and have no structural
370 correlation. Recently the cardinal pH and a_w models were successfully used to fit on experimental
371 data of *Salmonella enterica* ser. Newport biofilm formation in TSB (Dimakopoulou-Papazoglou et

372 al., 2016). To our knowledge, no data are available on the effects of environmental factors on *S.*
373 *aureus* biofilm formation. Therefore, herein both CPM and CPMI were effectively fitted to a data
374 set of *S. aureus* strain ATCC 13150. With the average goodness-of-fit index value close to 1.0, the
375 cardinal parameters and predicted biofilm formations were almost similar to experimentally
376 observed biofilm formation, indicating that the predictive biofilm formation models were accurate
377 for all condition used in the present study. Regarding goodness of fit statistic and prediction
378 accuracy, CPM gave a better quality fit compared to CPMI for *S. aureus* biofilm formation
379 irrespective of the environmental factors used in this study.

380 Individual-based modelling is an approach to understand and predict the processes that lead
381 to the development of microbial populations (spoilages and pathogens). Currently the use of cardinal
382 parameter models allows to describe the effects of environment factors (pH, EtOH, and a_w) on the
383 switching between planktonic and biofilm modes. The results demonstrated that the *S. aureus*
384 produced stronger biofilms at pH and a_w values close to optimal conditions of growth. The weak
385 biofilm formation was found within the range of pH and a_w that does not allow *S. aureus* growth.
386 Furthermore, the high biofilm production depended closely on the population growth of *S. aureus*.
387 Dimakopoulou-Papazoglou et al. (2016) studied the effect of pH and a_w on biofilm formation ability
388 of *Salmonella enterica* and concluded that biofilm formation required a similar range of pH and a_w
389 as needed for *Salmonella enterica* growth. It has been reported that the addition of NaCl in the
390 growth medium stimulated staphylococcal biofilm formation (Knobloch et al., 2001; Lim et al.,
391 2004; Møretrø et al., 2003). However, herein high percentages of NaCl interfered with bacterial
392 growth and biofilm formation. For EtOH, the higher biofilm formation may be due to a stress
393 response induced by ethyl alcohol at the non-lethal concentration. The concentration range of 2.5–
394 3.5 % of EtOH slightly interfered with the *S. aureus* growth because N_{max} at these concentrations
395 was lower than observed at 0.0% of EtOH. Therefore, a concentration range of 2.5–3.5 % was found
396 as non-lethal concentrations activating a stronger biofilm formation in *S. aureus* strain 13150. A
397 number of studies have reported that treatments with low concentrations of alcohols can enhance
398 the formation of staphylococcal biofilm. Korem et al. (2010) studied the hemolytic effect induced
399 by alcohols and they reported that ethanol (2.4 %) increased the expression of multiple surface
400 proteins, which might be important for cell attachment. Redelman et al. (2012) proved that different

401 alcohols (ethanol, isopropanol, methanol...) induced stress which significantly affected *S. aureus*
402 biofilm formation, partly through enhanced production of extracellular matrix and other biofilm-
403 promoting factors (Archer et al., 2011). In the future, it will be interesting to move this research
404 forward to include other alcohols commonly used as sanitizers in the food industry and hospitals.

405 In order to see whether the *S. aureus* growth is correlated with an increase in biofilm
406 formation a combination of the Baranyi and Roberts (1994) model and a linear model described by
407 (Castelijn et al., 2012; Kadam et al., 2013) was applied to calculate the growth parameters and the
408 factor *a*. The results showed a clear correlation between the growth parameters and biofilm
409 formation. Low lag time, high growth rate and maximum population density was associated with
410 high biofilm formation irrespective of the environmental conditions used in this study. The bacterial
411 density is of relevance as attached biofilm cells can contaminate foods during processing. The risk
412 of *S. aureus* biofilm formation would thus greatly dependent on bacterial population density and
413 stress conditions induced by nonlethal concentrations of ethanol. This result indicates that *S. aureus*
414 populations survive on food processing equipment and low concentrations of ethanol remaining
415 after disinfection may constitute a potential risk of biofilm formation under environmental stress,
416 therefore increasing the food safety risk.

417

418 **5. Conclusion**

419 The present study developed and validated a predictive model to quantitatively assess the
420 effects of pH, EtOH, and a_w on the biofilm formation ability of *S. aureus*. The developed cardinal
421 models allow defining the range of environmental factors for which the biofilm formation is
422 probable. These models were able to estimate the rate of *S. aureus* biofilm formation. Subsequently
423 these models can play a great role in risk assessment. The models are based on simplified growth
424 media and refer to indirect (optical density) biofilm formation measurements. Therefore, more
425 information about biofilm development on real food matrices and industrial food relevant surfaces
426 will permit optimization of their risk assessment.

427

428 **6. Acknowledgments**

429

430 This research was supported by a research grant of Kangwon National University 2015,
431 project PFV/10/002 (Center of Excellence OPTEC-Optimization in Engineering) of the KU Leuven
432 Research Council, projects G093013N of the Fund for Scientific Research-Flanders, and the Belgian
433 Program on Interuniversity Poles of Attraction, initiated by the Belgian Federal Science Policy
434 Office.

435 **References**

436

437 Akkermans, S., Fernandez, E.N., Logist, F., Van Impe, J.F., 2017. Introducing a novel interaction
438 model structure for the combined effect of temperature and pH on the microbial growth
439 rate. *Int. J. Food Microbiol.* 240, 85–96

440 Archer, N.K., Mazaitis, M.J., Costerton, J.W., Leid, J.G., Powers, M.E., Shirtliff, M.E., 2011.
441 *Staphylococcus aureus* biofilms: properties, regulation, and roles in human disease.
442 *Virulence* 2, 445-459.

443 Arciola, C.R., Campoccia, D., Speziale, P., Montanaro, L., Costerton, J.W., 2012. Biofilm formation
444 in *Staphylococcus* implant infections. A review of molecular mechanisms and implications
445 for biofilm-resistant materials. *Biomaterials* 33, 5967-5982.

446 Arrizubieta, M.J., Toledo-Arana, A., Amorena, B., Penadés, J.R., Lasa, I., 2004. Calcium inhibits
447 bap-dependent multicellular behavior in *Staphylococcus aureus*. *J. Bacteriol.* 186, 7490-
448 7498.

449 Baranyi, J., Roberts, T.A., 1994. A dynamic approach to predicting bacterial growth in food. *Int. J.*
450 *Food microbiol.* 23, 277-294.

451 Borucki, M.K., Peppin, J.D., White, D., Loge, F., Call, D.R., 2003. Variation in biofilm formation
452 among strains of *Listeria monocytogenes*. *Appl. Environ Microbiol.* 69, 7336-7342.

453 Bridier, A., Sanchez-Vizueté, P., Guilbaud, M., Piard, J.C., Naitali, M., Briandet, R., 2015. Biofilm-
454 associated persistence of food-borne pathogens. *Food Microbiol.* 45, 167-178.

455 Castelijin, G.A., van der Veen, S., Zwietering, M.H., Moezelaar, R., Abee, T., 2012. Diversity in
456 biofilm formation and production of curli fimbriae and cellulose of *Salmonella*
457 Typhimurium strains of different origin in high and low nutrient medium. *Biofouling* 28,
458 51-63.

459 da Silva Meira, Q.G., de Medeiros Barbosa, I., Athayde, A.J.A.A., de Siqueira-Júnior, J.P., de
460 Souza, E.L., 2012. Influence of temperature and surface kind on biofilm formation by
461 *Staphylococcus aureus* from food-contact surfaces and sensitivity to sanitizers. *Food Contr.*
462 25, 469-475.

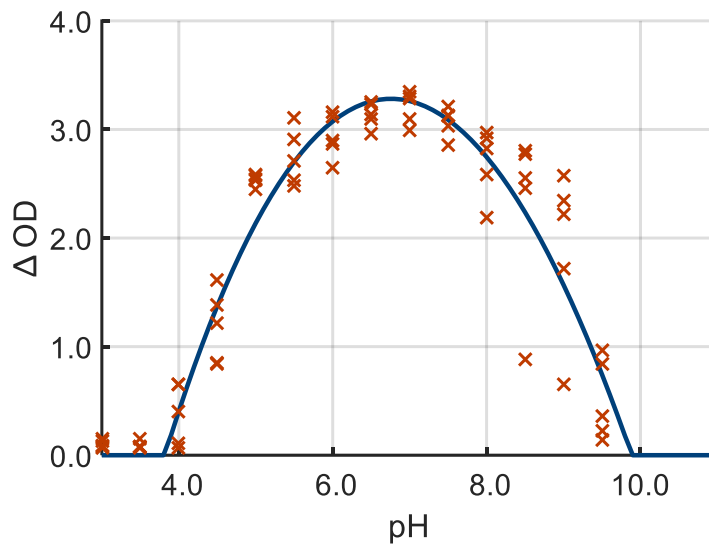
- 463 Dimakopoulou-Papazoglou, D., Lianou, A., Koutsoumanis, K.P., 2016. Modelling biofilm
464 formation of *Salmonella enterica* ser. Newport as a function of pH and water activity. Food
465 microbiology 53, 76-81.
- 466 Djordjevic, D., Wiedmann, M., McLandsborough, L., 2002. Microtiter plate assay for assessment
467 of *Listeria monocytogenes* biofilm formation. Appl. Environ. Microbiol. 68, 2950-2958.
- 468 Flemming, H.-C., Wingender, J., 2010. The biofilm matrix. Nature Rev. Microbiol. 8, 623-633.
- 469 Fox, L., Zadoks, R., Gaskins, C., 2005. Biofilm production by *Staphylococcus aureus* associated
470 with intramammary infection. Veter. Microbiol. 107, 295-299.
- 471 Gormley, F., Little, C., Rawal, N., Gillespie, I., Lebaigue, S., Adak, G., 2011. A 17-year review of
472 foodborne outbreaks: describing the continuing decline in England and Wales (1992–
473 2008). Epidemiol. Infect. 139, 688-699.
- 474 Gustafson, J.E., Muthaiyan, A., Dupre, J.M., Ricke, S.C., 2014. *Staphylococcus aureus* and
475 understanding the factors that impact enterotoxin production in foods: A Rev Food Contr.
476 (withdrawn from journal).
- 477 Gutiérrez, D., Delgado, S., Vázquez-Sánchez, D., Martínez, B., Cabo, M.L., Rodríguez, A., Herrera,
478 J.J., García, P., 2012. Incidence of *Staphylococcus aureus* and analysis of associated
479 bacterial communities on food industry surfaces. Appl. Environ. Microbiol. 78, 8547-8554.
- 480 Hermanowicz, S.W., 2001. A simple 2D biofilm model yields a variety of morphological features.
481 Mathemat. Biosc. 169, 1-14.
- 482 Hussain, M.S., Oh, D.H., 2017. Substratum attachment location and biofilm formation by *Bacillus*
483 *cereus* strains isolated from different sources: Effect on total biomass production and
484 sporulation in different growth conditions. Food Contr. 77, 270-280.
- 485 Kadam, S.R., den Besten, H.M., van der Veen, S., Zwietering, M.H., Moezelaar, R., Abee, T., 2013.
486 Diversity assessment of *Listeria monocytogenes* biofilm formation: impact of growth
487 condition, serotype and strain origin. Int. J. Food Microbiol. 165, 259-264.
- 488 Knobloch, J.K.M., Bartscht, K., Sabottke, A., Rohde, H., Feucht, H.H., Mack, D., 2001. Biofilm
489 formation by *Staphylococcus epidermidis* depends on functional RsbU, an activator of
490 the sigB operon: differential activation mechanisms due to ethanol and salt stress. J.
491 Bacteriol. 183, 2624-2633.

- 492 Korem, M., Gov, Y., Rosenberg, M., 2010. Global gene expression in *Staphylococcus aureus*
493 following exposure to alcohol. *Microbial Pathogen*. 48, 74-84.
- 494 Lim, Y., Jana, M., Luong, T.T., Lee, C.Y., 2004. Control of glucose-and NaCl-induced biofilm
495 formation by *rbf* in *Staphylococcus aureus*. *J. Bacteriol.* 186, 722-729.
- 496 Monds, R.D., O'Toole, G.A., 2009. The developmental model of microbial biofilms: ten years of a
497 paradigm up for review. *Trends in Microbiol.* 17, 73-87.
- 498 Møretrø, T., Hermansen, L., Holck, A.L., Sidhu, M.S., Rudi, K., Langsrud, S., 2003. Biofilm
499 formation and the presence of the intercellular adhesion locus *ica* among staphylococci
500 from food and food processing environments. *Appl. Environ. Microbiol.* 69, 5648-5655.
- 501 Perez-Rodriguez, F., Posada-Izquierdo, G., Valero, A., García-Gimeno, R., Zurera, G., 2013.
502 Modelling survival kinetics of *Staphylococcus aureus* and *Escherichia coli* O157: H7 on
503 stainless steel surfaces soiled with different substrates under static conditions of
504 temperature and relative humidity. *Food Microbiol.* 33, 197-204.
- 505 Planchon, S., Gaillard-Martinie, B., Dordet-Frisoni, E., Bellon-Fontaine, M., Leroy, S., Labadie, J.,
506 Hébraud, M., Talon, R., 2006. Formation of biofilm by *Staphylococcus xylosum*. *Int. J. Food*
507 *Microbiol.* 109, 88-96.
- 508 Redelman, C.V., Maduakolam, C., Anderson, G.G., 2012. Alcohol treatment enhances
509 *Staphylococcus aureus* biofilm development. *FEMS Immunol. Medical Microbiol.* 66, 411-
510 418.
- 511 Rode, T.M., Langsrud, S., Holck, A., Møretrø, T., 2007. Different patterns of biofilm formation in
512 *Staphylococcus aureus* under food-related stress conditions. *Int. J. food microbiol.* 116,
513 372-383.
- 514 Rohde, H., Burandt, E.C., Siemssen, N., Frommelt, L., Burdelski, C., Wurster, S., Scherpe, S.,
515 Davies, A.P., Harris, L.G., Horstkotte, M.A., 2007. Polysaccharide intercellular adhesin or
516 protein factors in biofilm accumulation of *Staphylococcus epidermidis* and *Staphylococcus*
517 *aureus* isolated from prosthetic hip and knee joint infections. *Biomaterials* 28, 1711-1720.
- 518 Ross, T., 1999. Predictive food microbiology models in the meat industry. *Meat and Livestock*
519 *Australia.*

- 520 Ross, T., Dalgaard, P., 2003. Secondary models. In: McKellar, Robin C, Lu, Xuewen (Eds.),
521 Modeling microbial responses in food. CRC series in contemporary food science. CRC
522 Press, pp. 63-134.
- 523 Rosso, L., Lobry, J.R., Flandrois, J.P., 1993. An unexpected correlation between cardinal
524 temperatures of microbial growth highlighted by a new model. J. Theor. Biol. 162, 447–
525 463.
- 526 Rosso, L., Lobry, J., Bajard, S., Flandrois, J., 1995. Convenient Model To Describe the Combined
527 Effects of Temperature and pH on Microbial Growth. Appl. Environ. Microbiol. 61, 610–
528 616.
- 529 Rosso, L., Robinson, T., 2001. A cardinal model to describe the effect of water activity on the
530 growth of moulds. Int. J. Food Microbiol. 63, 265-273.
- 531 Sharma, M., Anand, S., 2002. Characterization of constitutive microflora of biofilms in dairy
532 processing lines. Food microbiol. 19, 627-636.
- 533 Shi, X., Zhu, X., 2009. Biofilm formation and food safety in food industries. Trends in Food Sc.
534 Technol. 20, 407-413.
- 535 Tango, C.N., Hong, S.S., Wang, J., Oh, D.H., 2015. Assessment of enterotoxin production and
536 cross-contamination of *Staphylococcus aureus* between food processing materials and
537 ready-to-eat cooked fish paste. J. Food Sc. 80, M2911–M2916.
- 538 Xavier, J., Picioreanu, C., Van Loosdrecht, M., 2004. Assessment of three-dimensional biofilm
539 models through direct comparison with confocal microscopy imaging. Water Sc. Technol.
540 49, 177-185.
- 541
- 542
- 543
- 544
- 545
- 546
- 547
- 548

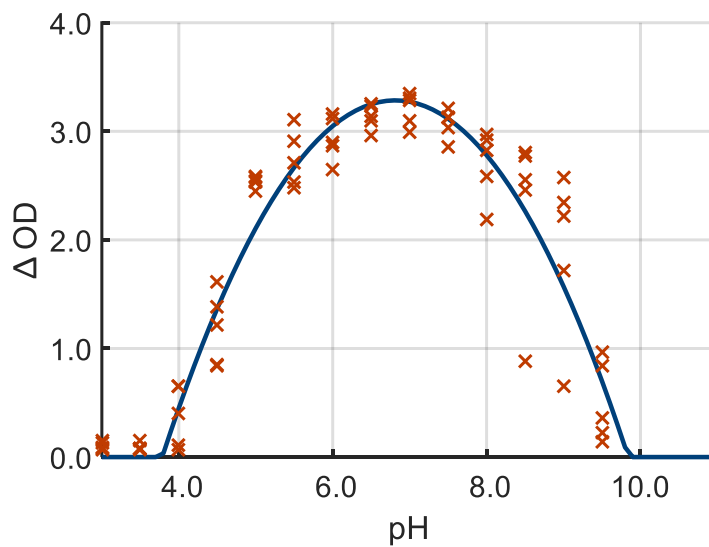
549 **FIGURES**

550 A



551

552 B



553

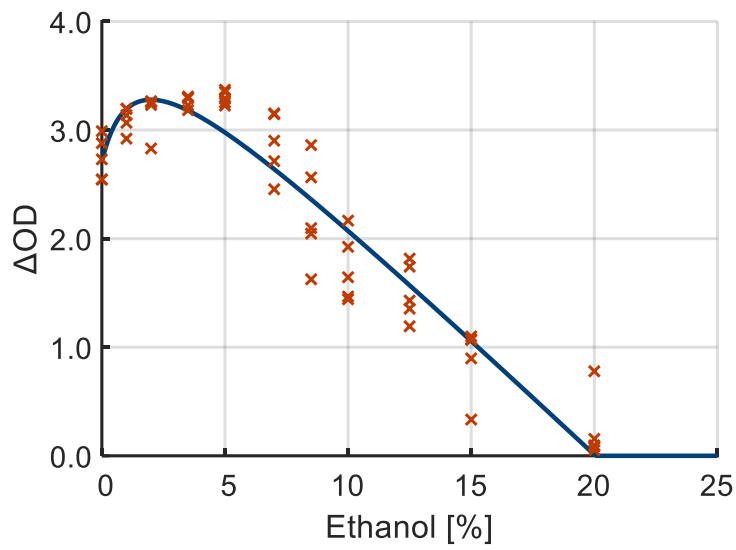
554 **Figure 1.** Cardinal parameter model for the effect of pH on *Staphylococcus aureus* biofilm

555 formation. A= cardinal parameter model, B= cardinal parameter model with inflection.

556

557

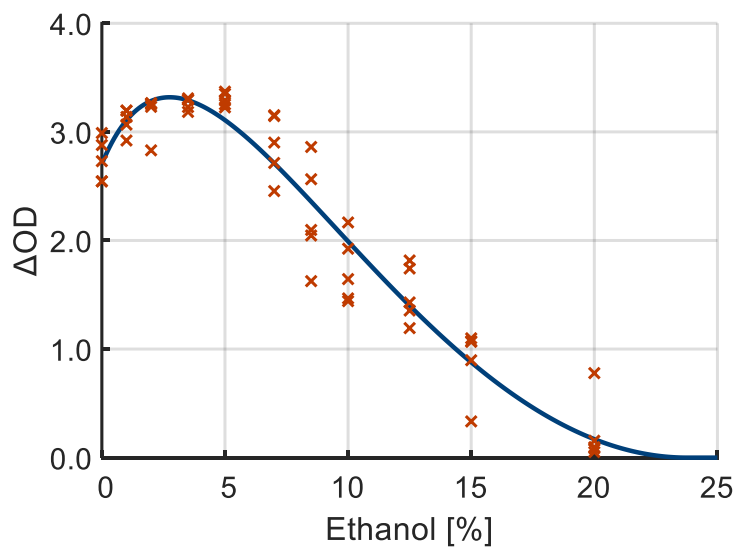
A



558

559

B



560

561

562 **Figure 2.** Cardinal parameter model for the effect of ethanol (%) on *Staphylococcus aureus*

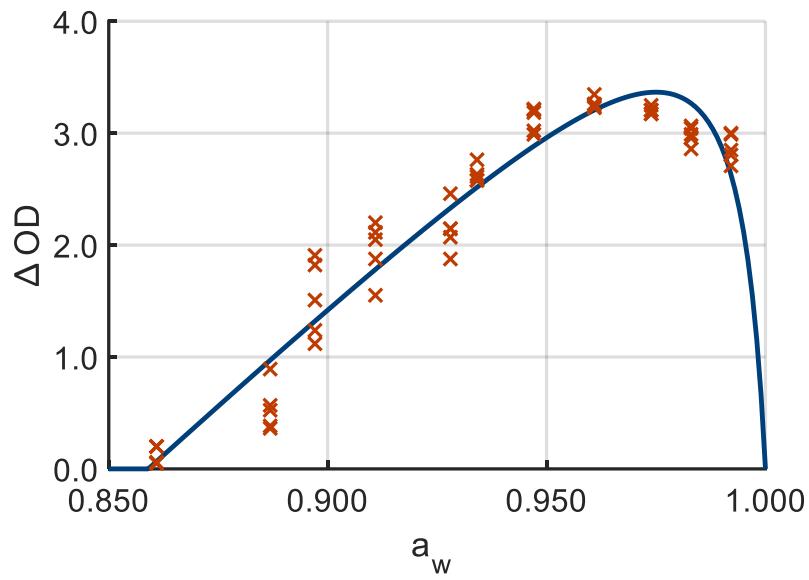
563 biofilm formation. A= cardinal parameter model, B= cardinal parameter model with inflection.

564

565

566

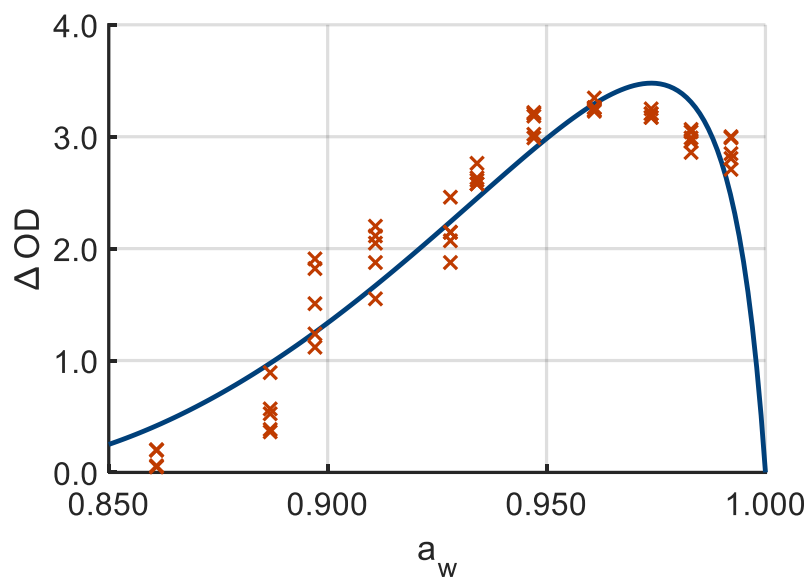
A



567

568

B



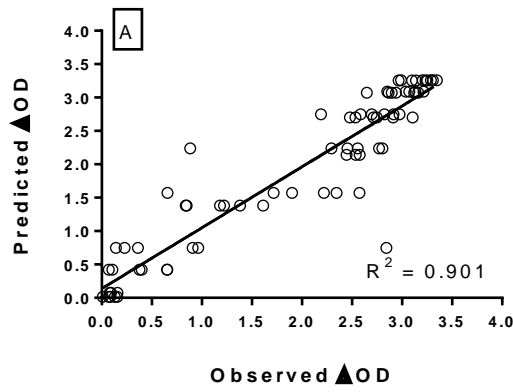
569

570

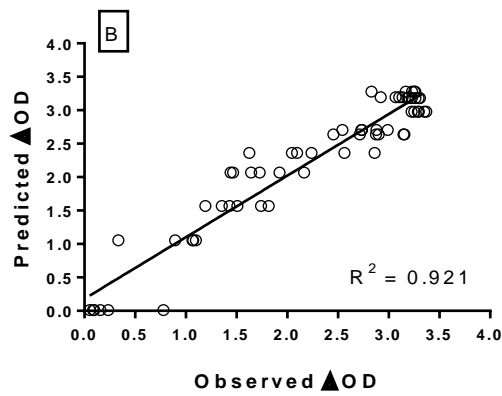
571

572

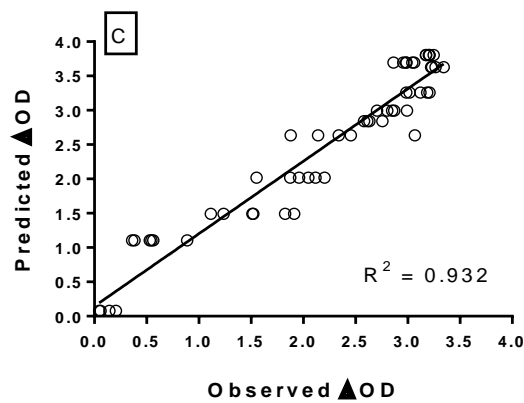
Figure 3. Cardinal parameter model for the effect of a_w on *Staphylococcus aureus* biofilm formation. A= cardinal parameter model, B= cardinal parameter model with inflection.



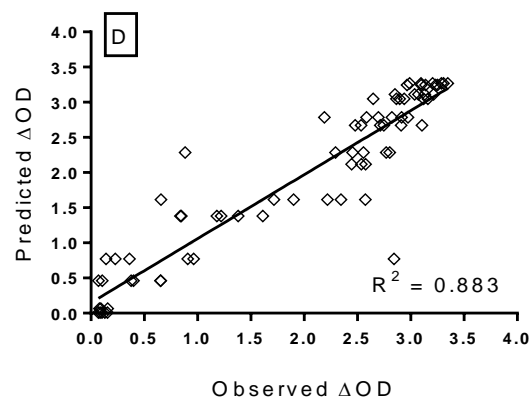
573



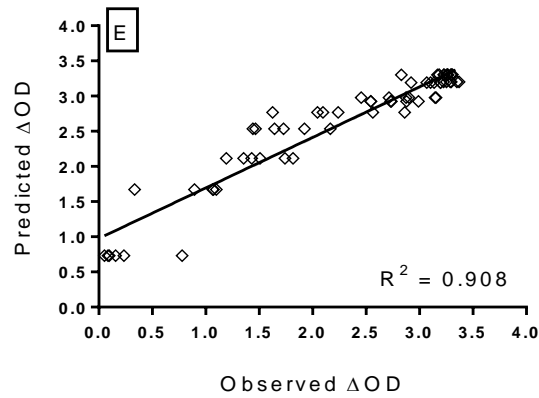
574



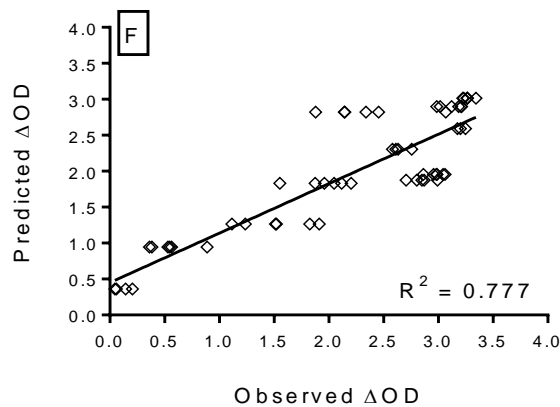
575



576



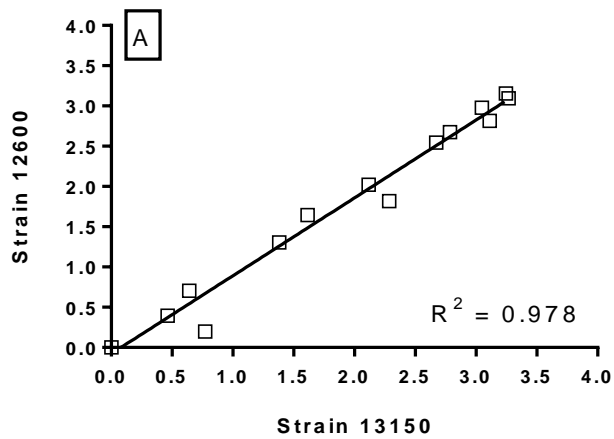
577



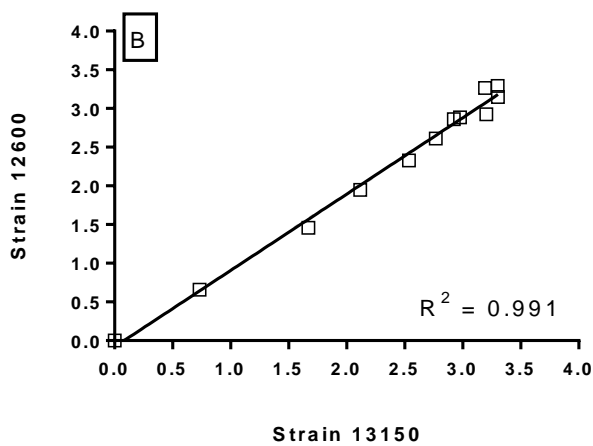
578

579 **Figure 4.** Comparison between predicted and observed ΔOD values for biofilm formation of
580 *Staphylococcus aureus* at various environmental conditions. Cardinal parameter model for pH (A),
581 cardinal parameter model for ethanol (B), cardinal parameter model for aw (C), cardinal parameter
582 model with inflection for pH (D), cardinal parameter model with inflection for ethanol (E), cardinal
583 parameter model with inflection for aw (F).

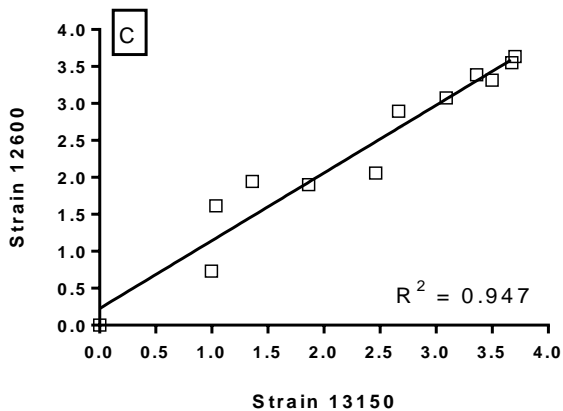
584



585



586



587

588 **Figure 5.** The correlation between the crystal violet staining assay and plate counts of
589 *Staphylococcus aureus*. Biofilm was formed in TSB with different pH (A), ethanol concentration
590 (B) and a_w (C) at 37 °C for 6 h–48 h. Absorbance values from the CV assay (OD590 nm) are plotted
591 against the log CFU/well and fitted with the linear equation.

592 **TABLES**

593

594 **Table 1.** Parameter estimates, with 95% confidence intervals (indicated with \pm) and goodness-of-fit statistic of CPM and CPMI describing the effect of pH,
 595 ethanol (% i.e. v/v), and a_w on ΔOD .

Factor	Parameter	CPM		Statistic	CPMI		Statistic
pH	pH _{min}	3.81	± 0.08	RMSE = 0.448	3.78	\pm 1.12	RMSE = 0.455
	pH _{opt}	6.76	± 0.10	B _f = 1.007	6.81	\pm 0.05	B _f = 1.222
	pH _{max}	9.89	± 0.11	A _f = 1.111	9.84	\pm 0.08	A _f = 1.311
	ΔOD_{opt}	3.28	± 0.07		3.28	\pm 0.08	
Ethanol	Eth _{min} (%)	0.93	± 0.97	RMSE = 0.317	-2.35	\pm 1.57	RMSE = 0.280
	Eth _{opt} (%)	1.99	± 0.67	B _f = 1.292	2.75	\pm 0.50	B _f = 0.771
	Eth _{max} (%)	20.05	± 1.14	A _f = 1.416	23.76	\pm 2.62	A _f = 1.303
	ΔOD_{opt}	3.27	± 0.17		3.32	\pm 0.15	
a_w	$a_{w,min}$	0.86	± 0.003	RMSE = 0.276	0.81	\pm 0.01	RMSE = 0.327
	$a_{w,opt}$	0.98	\pm 0.001	B _f = 1.021	0.97	\pm 0.001	B _f = 0.996
	ΔOD_{opt}	3.37	± 0.06	A _f = 1.293	3.48	\pm 0.07	A _f = 1.344

596 CPM: Cardinal parameter models; CPMI: Cardinal parameter models inflection. RMSE: Root Mean Square Error; B_f: Bias factor; A_f: Accuracy factor.

597

598 **Table 2.** Parameter a estimated from equation (6) and growth parameters from Baranyi and Roberts model.

Factor	Condition	a	Growth parameters			R^2_{adj}
			r_{max}	λ	N_{max}	
pH	4.00	$7.88 \times 10^{-8}b$	0.058a	14.56d	6.14b	0.989
	5.50	$1.76 \times 10^{-6}c$	0.172b	5.15c	8.86c	0.987
	7.00	$2.85 \times 10^{-6}d$	0.249c	2.45a	9.04d	0.986
	8.50	$1.83 \times 10^{-6}c$	0.224c	3.67b	8.96cd	0.997
	9.50	$6.59 \times 10^{-8}a$	0.034a	18.55a	4.94a	0.839
Ethanol (%)	0.0	$2.12 \times 10^{-6}c$	0.284d	3.81a	9.45d	0.987
	3.5	$3.55 \times 10^{-6}d$	0.164c	5.01b	8.84c	0.990
	7.0	$2.91 \times 10^{-6}e$	0.155c	5.47b	8.91c	0.994
	12.5	$5.55 \times 10^{-7}b$	0.110b	13.6c	7.88b	0.988
	20.0	$1.66 \times 10^{-7}a$	0.041a	20.9d	6.95a	0.967
a_w	0.99	$1.75 \times 10^{-6}c$	0.289d	3.95a	9.46d	0.997
	0.98	$2.77 \times 10^{-6}d$	0.235c	4.08ab	9.31c	0.871
	0.96	$3.15 \times 10^{-6}e$	0.233c	4.20b	9.15c	0.901
	0.93	$9.89 \times 10^{-7}b$	0.164b	14.14c	7.76b	0.938
	0.88	$2.22 \times 10^{-8}a$	0.059a	16.63d	6.48a	0.974

599 a : proportionality constant between CV staining and cell counts, r_{max} : maximum growth rate (1/h); λ : Lag time (hour); N_{max} : maximum population density (log
 600 cfu/well). Different letters in the same column indicate significant differences ($p < 0.05$) for estimated parameters.

601